

Formation of C=C Bond via Knoevenagel Reaction between Aromatic Aldehyde and Barbituric Acid at Liquid/HOPG and Vapor/HOPG Interfaces

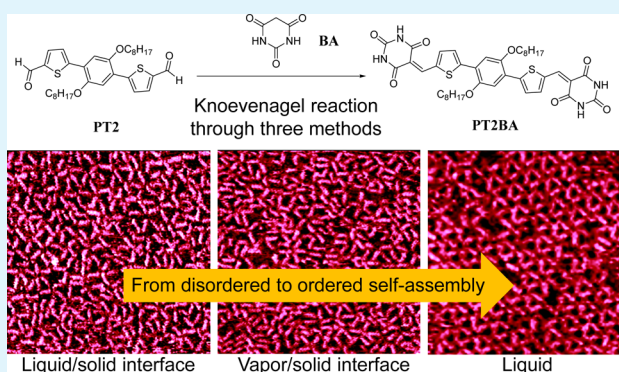
Yanfeng Geng, Hongliang Dai, Shaoqing Chang, Fangyun Hu, Qingdao Zeng,* and Chen Wang*

CAS Key Laboratory of Standardization and Measurement for Nanotechnology, National Center for Nanoscience and Technology, No. 11 Beiyitiao, Zhongguancun, Beijing 100190, P. R. China

S Supporting Information

ABSTRACT: Controlling chemical reactions on surface is of great importance to constructing self-assembled covalent nanostructures. Herein, Knoevenagel reaction between aromatic aldehyde compound 2,5-di(5-aldehyde-2-thienyl)-1,4-dioctyloxybenzene (PT2) and barbituric acid (BA) has been successfully performed for the first time at liquid/HOPG interface and vapor/HOPG interface. The resulting surface nanostructures and the formation of C=C bond are recorded through scanning tunneling microscopy (STM), and confirmed by attenuated total reflectance Fourier-transform infrared (ATR/FT-IR) spectrometer and UV-vis absorption. The obtained results reveal that Knoevenagel condensation reaction can efficiently occur at both interfaces. This surface reaction would be an important step toward further reaction to produce innovative conjugated nanomaterial on the surface.

KEYWORDS: C=C bond, Knoevenagel reaction, interface



INTRODUCTION

The bottom-up self-assembly is one of the most studied approaches to obtaining nanostructures with controlled dimensions and innovational properties.^{1–3} Although the self-assemblies driven by weak and reversible interaction (van der Waals forces, hydrogen bonding, coordination bond, and so on) are well-developed nanostructures in large scale, they are very fragile and easy to collapse under special conditions (high temperature, low pressure, air and water exposure).^{4–6} In a sense, these equilibrium self-assembled structures driven by noncovalent bonds have poor mechanical and chemical stability, and can not be applied extensively. Control of molecular arrangement is the prerequisite for their potential application in nanotechnology development. Therefore, it is very necessary to obtain mechanically and chemically stable functional nanostructures with controlled dimensions.

It is important to explore surface reaction in order to construct stable nanostructures on the surface.^{7–11} Similar with the solution reactions, on-surface chemical reactions involve breakage and formation of chemical bonds. New compounds could be obtained by the in situ synthesis on the surface.^{12–14} In the recent years, enormous effort has been devoted into the in situ formation of covalent bonds to construct covalently interlinked organic molecular nanostructures on various surfaces or interfaces.^{3,15–19} The covalent bonds include N–H, C–C, B–O, C=N, C–N, and so on, based on the electron

transfer reaction,²⁰ photochemical reaction,^{21,22} Ullmann coupling reaction,^{23,24} Glaser coupling reaction,^{25–27} boronic acid condensation reaction,²⁸ Schiff-base coupling reaction,^{29,30} condensation reaction between acyl chlorides and amines,^{31,32} etc. The photochemical reaction usually occurs within the monolayer of photoactive molecules.³³ Ullmann coupling is an organic reaction of two haloaromatics to form a biaromatic molecule via catalyst. The dehydration reaction of boronic acid can form boron linked molecule and construct covalent nanostructures.³⁴ Imine-based molecules can be formed through Schiff-base coupling reaction between aldehydes and amines.³⁵ The strong and irreversible covalent bond has been considered as a promising alternative for fabricating thermodynamically stable self-assembled materials on the surfaces. A large number of zero-dimension (0D), one-dimension (1D), and two-dimension (2D) large-scale covalent structures with the help of various surface reactions have been achieved.^{36–39}

Nevertheless, experimental studies aimed at creating and characterizing conjugated molecules have not been widely devoted.⁴⁰ Conjugated bond in 2D may enhance carrier mobility or other favorable properties and extend the application of molecule device. To explore versatile application

Received: November 18, 2014

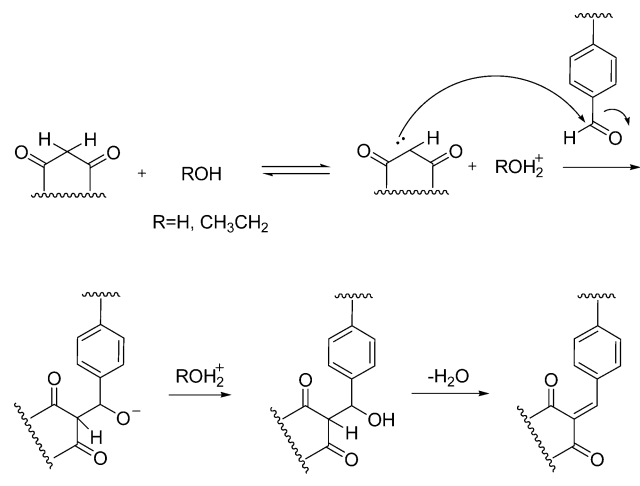
Accepted: February 9, 2015

Published: February 9, 2015

of conjugated molecules, it is particularly interesting to study the reaction which can directly form alkene linkage on the surface. Up to now, no reaction directly generating C=C alkene groups on the surface has been reported. Thus, it is very important to investigate the reaction process as well as self-assembled properties of the final nanostructures. In particular, the incorporation of alkene bonds can offer conjugation sites in organic semiconductors, and thus might be utilized as efficient building block for semiconducting polymers.

Alkenes can be prepared by elimination reaction, reduction reaction and condensation reaction in the solution. Knoevenagel condensation reaction has been considered as an important reaction for generating C=C double bond. This reaction is really a nucleophilic addition of an active-methylene-containing compound to a carbonyl group and finally can generate C=C double bond in water or ethanol condition, in which a molecule of water is eliminated.⁴¹ A proposed mechanism is shown in Scheme 1. So far, the study of Knoevenagel condensation

Scheme 1. Proposed Mechanism of Knoevenagel Condensation Reaction for the Formation of Double Bond under H₂O (R = H) or CH₃CH₂OH (R = CH₃CH₂) Conditions



reaction on the highly oriented pyrolytic graphite (HOPG) surface is rarely reported, which is crucial to understand the surface chemical reaction and to develop 2D conjugated nanomaterials and further electronic nanodevices. Two kinds of methods (liquid and vapor) were used to understand the process of Knoevenagel reaction on the surface.⁴² At liquid/HOPG interface, ethanol was used as the solvent, whereas CuSO₄·5H₂O was used in the case of vapor/HOPG interface.

Barbituric acid (BA) is selected as monomers because BA not only provides active methylene for reaction but also supplies amine groups to create hydrogen-bonding for the formation of supramolecular assemblies with a high degree of symmetries.^{43–46} On the other hand, a previously reported aromatic aldehyde compound, 2,5-di(5-aldehyde-2-thienyl)-1,4-dioctyloxybenzene (PT2) was employed as an aldehyde functionalized monomer.³⁰ The self-assembled properties of presynthesized PT2BA and the surface nanostructures after in situ reaction have been characterized by scanning tunnelling microscopy (STM), which can provide insight into the surface reactions on the molecular scale as well as the morphology of self-assembled nanostructures on the surfaces. The chemical bonds as well as the in situ reaction conversion have been

confirmed via attenuated total reflectance Fourier-transform infrared experiments (ATR/FT-IR) and UV–vis absorption. The reacted and unreacted statuses of the intermediates have also been discussed according to the adsorption geometry.

EXPERIMENTAL SECTION

Materials. The reactant PT2 was prepared according our previous report.³⁰ The compound PT2BA was obtained through thermal treatment in ethanol solution, and the detailed procedure is shown in the Supporting Information. The freshly cleaved HOPG (grade ZYB, NTMDT, Russia) was used as the substrate.

Sample Preparation. PT2 sample was prepared by depositing ethanol solution with concentration of 10^{−4} M onto the HOPG surface. The PT2BA sample was prepared by depositing a droplet (0.4 μL) of tetrahydrofuran solution with the concentration less than 1 × 10^{−4} M onto the HOPG surface. The surface reaction between PT2 and BA was conducted at liquid/HOPG and vapor/HOPG interfaces. After preparation of sample, a droplet (0.1 μL) of pure solvent 1-phenylacetone was added onto these surfaces before STM measurement.

Surface Reaction. At liquid/HOPG interface: a droplet (0.4 μL) of ethanol solution containing PT2 and barbituric acid with the concentration less than 1 × 10^{−4} M was applied into HOPG surface. Then, the sample was annealed at 60 °C in ethanol for 12 h. Analytical reagent ethanol was ceaselessly added onto the sample in order to keep the reaction happened at atmosphere of ethanol. At vapor/HOPG interface: a droplet of PT2 ethanol solution (1 × 10^{−4} M) was deposited onto the freshly cleaved HOPG surface and dry for several minutes. After that, HOPG sample, BA (ca. 0.2 mg) and CuSO₄·5H₂O powder (ca. 1.2 g) were added to the bottom of custom-built Teflon-sealed autoclave. The autoclave was sealed and put into a heating oven at 150 °C for 3 h to finish the surface reaction.

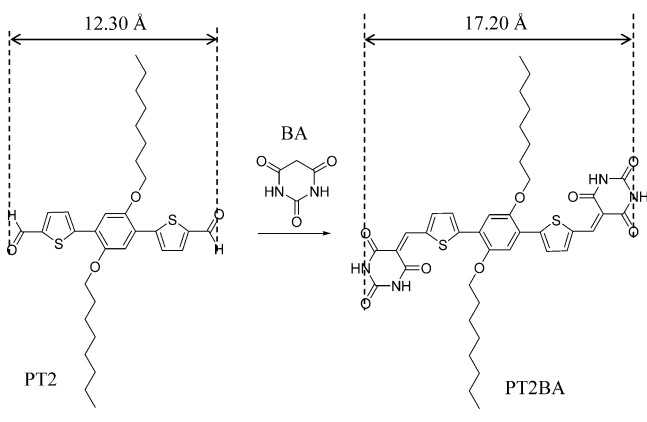
Characterization. The STM experiments were carried out in a Nanoscope IIIa (Bruker, USA) under atmosphere conditions. The STM images presented were acquired in constant current mode using a mechanically formed Pt/Ir (80/20) tip. All STM images provide were raw data without ant treatment expect for the flattening procession and the drift was calibrated using the underlying graphite lattice as a reference. The specific tunneling conditions including tunneling current (*I*_{set}) and sample bias (*V*_{bias}) are given in the corresponding figure captions throughout the article. The molecular models were built with a HyperChem software package. The density functional theory (DFT) provided by DMol3 code was conducted to estimate the length of molecules. Attenuated total reflectance Fourier-transform infrared (ATR/FT-IR) spectra were carried out and Excalibur 3100 spectrometer (Varian, USA) equipped with ATR accessory was employed. The resolution was 0.20 cm^{−1}, whereas 64 scans were set to obtain each spectrum in the region from 600 to 3500 cm^{−1}. UV–vis absorption spectra were measured using a UV-756 spectrometer.

RESULTS AND DISCUSSION

Self-Assembly of Presynthesized PT2BA. The self-assembly of dialdehyde precursor PT2 was performed in order to confirm the geometry and chemical change after ex situ and in situ reactions. A representative STM image similar to our previous report,³⁰ in which heptanoic acid is used for liquid/solid interface was shown in Figure S1 in the Supporting Information. The arranged bright rectangles correspond to the core of PT2 molecules and the alkoxy chains lie in the dark channel. The length (*L*) of the bright rectangles was statistically estimated to be 1.1 ± 0.2 nm.

The compound PT2BA was presynthesized via Knoevenagel reaction by thermal solvent method as shown in Scheme 2. The theoretical calculation was performed by using density functional theory (DFT) to estimate the length of PT2 and PT2BA molecules to be 1.23 and 1.72 nm, respectively. The

Scheme 2. Reaction Route of PT2BA with Molecular Length Estimated from Calculations Using the Density Functional Theory (DFT) Provided by DMol3 Code



calculated lengths are slightly larger than the estimated length from the STM images because the former is the distance of atoms, whereas the latter is the estimation results according to the cloud density shown in STM images. Regardless, this geometry change could give much information on the surface reaction.

Deposition of PT2BA solution onto HOPG surface resulted in well-ordered structure, and the characterization of the molecular nanostructures was carried out by utilizing STM at room temperature. Figure 1 shows a representative large-scale STM image. The presynthesized PT2BA molecules appeared as bright rods on the surface, and the average length is estimated to be 1.6 ± 0.2 nm. Six PT2BA molecules make up a flowerlike

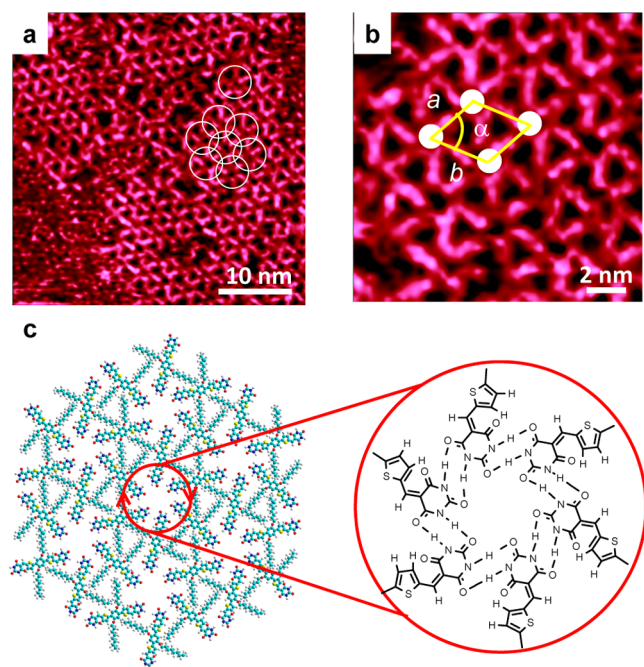


Figure 1. (a) Large-scale STM image of PT2BA self-assembled monolayer at the 1-phenyloctane/HOPG surface with circles marking flower-structure containing six PT2BA molecules on the surface. (b) A close-up image of the PT2BA self-assemblies. (c) A suggested structural model for the network on HOPG. Inset illuminates the intermolecular hydrogen bonds as indicated by dotted lines. Imaging conditions: $I_{\text{set}} = 820$ pA, $V_{\text{bias}} = 380$ mV.

structure as marked by white circles and one circle was symmetrically surrounded by six circles. The obtained symmetrical assembled structure indicates strong intermolecular interaction for PT2BA molecules on the HOPG surface. With close inspection of high-resolution STM image, six PT2BA molecules closely connect with each other to form a cavity with diameter of 1.0 ± 0.1 nm. The parameters of unit cell are measured to be $a = b = 3.2 \pm 0.1$ nm and $\alpha = 60 \pm 2^\circ$, respectively. Moreover, it can be found that PT2BA shows clockwise rotation, whereas no opposite chirality was found. Molecular model based on STM image is shown in Figure 1c. The resulted networks are proposed to be constructed by hydrogen bond between the terminal groups, indicating the strong intermolecular interaction due to the presence of barbituric acid.^{47,48} Therefore, PT2BA molecules self-assemble to network through hydrogen bonds between amine group and carbonyl group in terminal barbituric acid units. In other words, the hydrogen bonds between the terminal barbituric acid groups of PT2BA molecules play an important role in the formation of self-assembled nanostructures.

In Situ Synthesis of PT2BA at the Interfaces. As shown in the proposed mechanism of Knoevenagel reaction, water or ethanol facilitated the deprotonating of barbituric acid monomer to form the corresponding carbon anion. The latter attacked the aldehyde group of PT2 monomer and formed the alcohol intermediate. The process of dehydration was followed to afford product PT2BA molecule. The Knoevenagel reaction of monomers PT2 and BA was conducted at liquid/HOPG interface and vapor/HOPG interface, respectively. Full experiment procedure can be seen in the Experimental Section.²⁷

In the case of liquid/HOPG, STM characterization as shown in Figure 2a reveals that the formed PT2BA is widespread across the surface in the large scale. Despite disordered morphology, there are clearly flowerlike structures as marked with white circles in large scale as same as the structure of presynthesized PT2BA on HOPG surface. The result indicates that Knoevenagel condensation reaction occurs at the liquid/HOPG interface. For a more detailed study of the reaction, the length of the bright worm-like molecules was estimated with the help of the STM software. From the statistical analysis result as shown in Figure 2b, the length of the wormlike molecules ranges from 1.1 to 2.2 nm. As theoretical calculation mentioned above, the length of 1.3 ± 0.2 nm wormlike molecules might be assigned to the intermediate, where PT2 reacted with only one barbituric acid. As shown in Figure 2b, it can be found that the product PT2BA shows abundance of up to 65%, which indicates the Knoevenagel reaction has great potential for application in the on-surface reaction field to construct future functional nanomaterials.

In the case of vapor/solid interface, an efficient method to accomplish on-surface chemical reaction was shown in the previous reports,^{34,49,50} and the feed ratio, the coverage of the precursor on HOPG, the reaction temperature and the reaction time have been changed to optimize the reaction condition occurring on the surface. Figure 3a shows a large-scale STM image of the reacted surface. The arranged bright short rectangle phases correspond to the unreacted PT2 molecules, whereas the wormlike molecules can be assigned to the obtained compounds. Similar to the liquid/HOPG interface method, flowerlike structures as marked with circles appeared in large scale, which indicates that product PT2BA molecules were synthesized at the vapor/HOPG interface. A reacted region as marked with a red square was selected, and the length

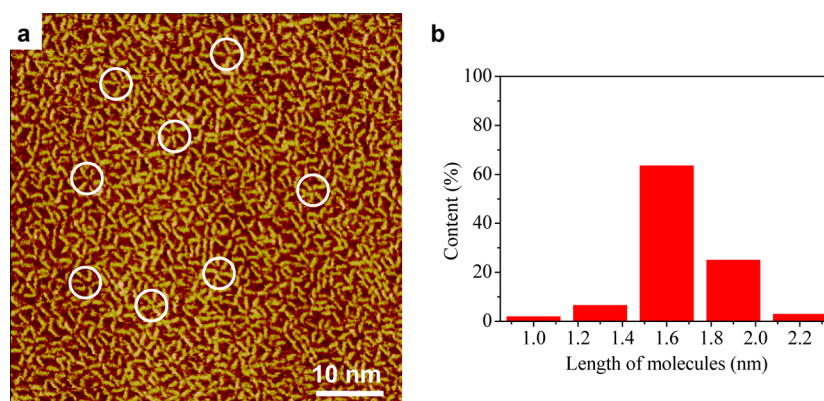


Figure 2. (a) Large-scale STM image of Knoevenagel reaction at liquid/HOPG interface. (b) The distribution of the length of molecules measured from the STM image. Imaging conditions for a: $I_{\text{set}} = 640$ pA, $V_{\text{bias}} = 410$ mV.

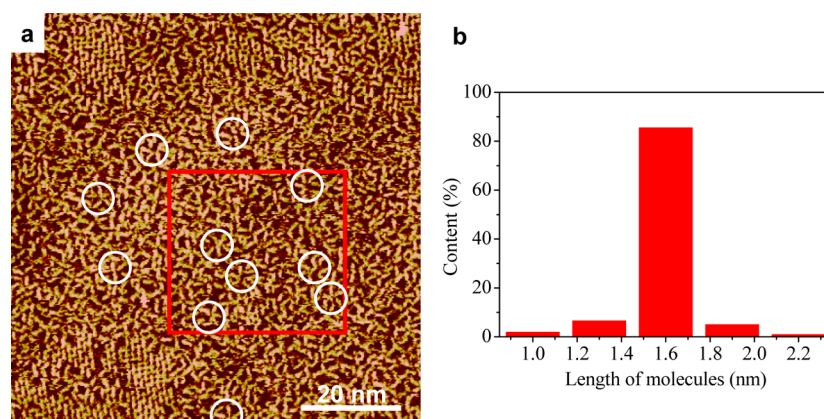


Figure 3. (a) Large-scale STM image of vapor/HOPG interface reaction. (b) Distribution of the length of molecules measured from the selected region marked with a red square in (a). Imaging conditions: $I_{\text{set}} = 320$ pA, $V_{\text{bias}} = 530$ mV.

Table 1. Proposed Hydrogen-Bonding Interaction Linkages of Wormlike Molecular with Length of Circa 1.9 nm from the STM Images^b

MC ^a	Form I	Form II
⌈		
⌋		

^aMolecular Conformation. ^bThe black curved lines correspond to the extending direction of complexes because of the intermolecular hydrogen-bonding interaction.

of bright wormlike molecules was calculated and the statistical result is shown in Figure 3b. The percentage of wormlike molecules with length of 1.6 ± 0.2 nm is up to 85%. The relative amount of 1.1 ± 0.2 nm molecules is about 6.5%.

It is worthwhile to note that the disordered structures at liquid/HOPG interface and at vapor/HOPG interface possibly result from the unreacted PT2, incomplete-reacted PT2, and the residual free barbituric acid coexisting on the surface. The

interaction between barbituric acid groups might restrict the mobility of barbituric acid on the surface to react with aldehyde group.⁵¹ These results reveal that the intermolecular hydrogen-bonding interaction is not strong enough to reorganize the single molecule after surface reaction. This is different from the covalent organic frameworks (COFs), which is stabilized by covalent interaction in the formed assembled structures.^{11,40,50,52} Therefore, intermolecular interaction could be

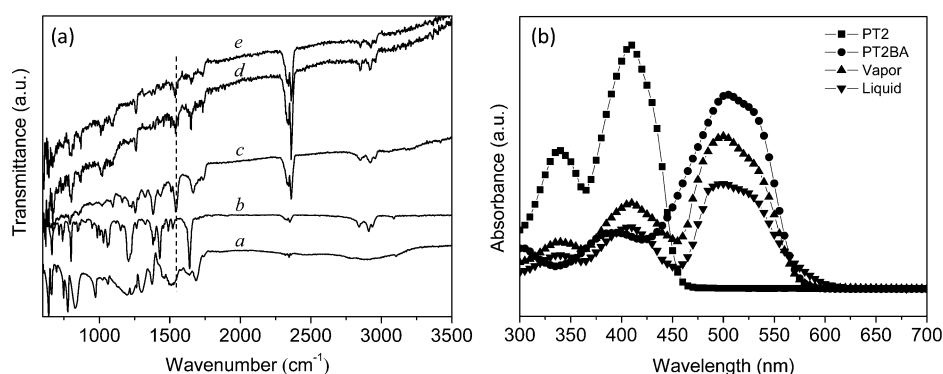


Figure 4. (a) ATR/FT-IR spectra in the region of 600–3500 cm^{-1} of the monomers (a) BA, (b) PT2, (c) the presynthesized PT2BA, (d) liquid/HOPG PT2BA, and (e) vapor/HOPG PT2BA, respectively. (b) UV-vis absorption spectra of PT2, presynthesized PT2BA, in situ vapor and liquid reaction.

a reaction barrier, which requires further experimental and theoretical investigation.

As shown in Figures 2b and 3b, STM images also clearly indicated the occurrence of molecules with length more than 1.6 ± 0.2 nm. What are these larger wormlike compounds? No other reactions could occur, therefore, there might be more complex interaction and molecular alignment. As shown in Figure 1, adjacent two terminal barbituric acids connect with each other through two hydrogen bonds. As a matter of fact, there might be another possible interaction form, in which two terminal barbituric acids connect with each other through only one hydrogen bond.

Table 1 shows two forms of interaction between barbituric acid groups. According to length of worm-like compounds, the features larger than 1.6 ± 0.2 nm can be attributed to different types of complexes with barbituric acid monomers. Importantly, both hydrogen bonds are parallel facing opposite directions in Form I, while only one hydrogen bond could result in an angle between molecules in the case of Form II. For the complexes with length of ca. 1.9 nm, it is possible that one unreacted BA molecule connected to the terminal barbituric acid group of one PT2BA molecule. Two terminal barbituric acid groups in one PT2BA molecule connected to two unreacted BA molecules to form complexes with length of ca. 2.1 nm.

According to the hydrogen-bonding linkage, there are several kinds of conformation, which is in accordance with the various wormlike molecules as shown in STM images. It is worth mentioning that the residual free amine and carbonyl groups on these complexes could provide other hydrogen-bonding interactions to form complicated dendritic structure. Additionally, although the interaction between aldehyde groups or aldehyde with other groups has been discussed,⁵³ the interaction is weaker compared with the hydrogen bonding between BA molecules and PT2BA terminal BA groups.^{29,54} We attempted to add BA and PT2 precursor to presynthesized PT2BA monolayer on HOPG surface to confirm the influence of unreacted BA and PT2 molecules on the self-assembled nanostructure. The STM images as shown in Figure S2 in the Supporting Information show similar morphology in Figures 2 and 3. Consequently, many hydrogen-bonding sites in barbituric acid group induce various types of intermolecular interactions.

Spectrum Analyses. To further confirm the occurrence of Knoevenagel reaction, ATR/FT-IR experiment was first carried out to study the molecular structure. Those samples for ATR/

FT-IR measurement were prepared as described in STM measurement. The ATR/FT-IR spectra of presynthesized PT2BA, on-surface synthesized PT2BA as well as monomers BA and PT2 are recorded and shown in Figure 4a. The peaks at 2853 and 2928 cm^{-1} are attributed to the C–H stretching of $-\text{CH}_2-$ and $-\text{CH}_3$.⁵⁵ The band at 2360 cm^{-1} corresponds to the N–H stretching.⁵⁶ The band at 1738 cm^{-1} is assigned to C–H aromatic stretching. The obtained band at 1659 cm^{-1} is due to the C=O stretching vibration. A C=C peak are observed at 1548 cm^{-1} after the ex situ or in situ reaction. The band around 1256 cm^{-1} is attributed to C–H bending vibrations. The band between 1010 and 1093 cm^{-1} corresponds to C–O–C stretching.⁵⁷ The band found at 869 cm^{-1} is assigned to the C–H bending absorption.⁵⁸ The band 668 cm^{-1} can be assigned to C–S absorption.⁵⁹ The new band at around 1548 cm^{-1} in spectrum of presynthesized PT2BA is associated with the generated C=C stretching mode. Compared with the presynthesized PT2BA, the obtained bands at 1546 cm^{-1} in spectra d (liquid/HOPG) and e (vapor/HOPG) are slightly weaker after surface reaction. Additionally, there are still monomer spectra at both spectra d and e, indicating the presence of monomers, which is in accordance with the STM results. Thus, these results confirm occurrence of Knoevenagel reaction at the interfaces, generation of C=C double bond and the presence of product PT2BA. The slight change in frequency might be due to the existing intermolecular hydrogen-bonding.⁶⁰

Moreover, UV-vis absorption spectra were recorded as shown in Figure 4b. It should be noted that precursor PT2 and presynthesized PT2BA were directly dissolved in THF solvent for UV-vis measurements. In the case of in situ reaction, the substrates after reaction were immersed in the solvent, and the obtained solutions were used for UV-vis absorption experiments. As shown in Figure 4b, PT2 shows two absorption peaks as observed at 338 and 407 nm. PT2BA solution shows two peaks at 385 and 501 nm. The maximum absorption is red-shifted by 94 nm compared with that of PT2, indicating an increasing of the conjugation due to the formation of C=C linkage.⁶¹ For the in situ reaction (vapor and liquid), the spectra show three peaks around 338, 407, and 501 nm, which indicate that PT2 and PT2BA coexist. Therefore, it can be concluded that the reaction happened after vapor and liquid reaction, although there is still PT2 molecules, which agrees with the result from STM and FTIR research.

From STM images, ATR/FT-IR and UV-vis absorption spectrum analyses, it can be concluded that the Knoevenagel

condensation reaction indeed successfully happened at liquid/HOPG and vapor/HOPG interfaces although large-scale ordered structure was not obtained. For the formation of well-defined complexes, appropriate hydrogen-bonding interaction should be designed. It is necessary to choose reactions and suitable reactants in order to take advantage of the interaction effects, especially for the nanostructure demanding hydrogen-bonding sites. The reaction between PT2 and another monomer, which has different chemical structure from barbituric acid, is going on for ordered structure. Further study will be continued on the surface reaction mechanism to construct large-scale ordered conjugated networks and explore the application in organic electronics and energy storage field. Based on this kind of reaction, chemical and surface researchers would develop many unprecedented structures and functional materials.

CONCLUSION

Presynthesized PT2BA compound can organize into self-assembled symmetrical structure on HOPG surface. Knoevenagel condensation reaction between aromatic aldehyde compound PT2 and BA was first conducted at both liquid/HOPG interface and vapor/HOPG interface. After the completion of interface reaction, high-resolution STM images and spectra analysis reveal that the Knoevenagel condensation reaction has been successfully achieved at both interfaces. Although unreacted PT2, intermediate, product PT2BA and species constructed through various hydrogen-bonding coexist on the HOPG surface, the amount of the product PT2BA is in the majority. The flowerlike structures as same as the presynthesized PT2BA on HOPG surface can also be obtained. Various intermolecular hydrogen-bonding interactions have been proposed to explain the observed complicated worm-like compounds. The intermolecular interactions played an important role in on-surface reaction for self-assembly nanostructures. This work observed a new surface reaction, and importantly provided valuable information about the interaction in the procedure of surface reaction and a new strategy for constructing surface-conjugated nanostructures.

ASSOCIATED CONTENT

Supporting Information

Synthesis of PT2BA and STM images. This material is available free of charge via the Internet at <http://pubs.acs.org>.

AUTHOR INFORMATION

Corresponding Authors

*E-mail: zengqd@nanocr.cn.

*E-mail: wangch@nanocr.cn.

Notes

The authors declare no competing financial interest.

ACKNOWLEDGMENTS

This work was supported by the National Basic Research Program of China (2011CB932303, 2013CB934200) and the National Natural Science Foundation of China (51173031, 91127043, 51203030, 21472029).

REFERENCES

(1) Palma, C. A.; Samori, P. Blueprinting Macromolecular Electronics. *Nat. Chem.* **2011**, *3*, 431–436.

(2) Ciesielski, A.; Palma, C. A.; Bonini, M.; Samori, P. Towards Supramolecular Engineering of Functional Nanomaterials: Pre-Programming Multi-Component 2D Self-Assembly at Solid-Liquid Interfaces. *Adv. Mater.* **2010**, *22*, 3506–3520.

(3) Gourdon, A. On-Surface Covalent Coupling in Ultrahigh Vacuum. *Angew. Chem., Int. Ed.* **2008**, *47*, 6950–6953.

(4) Kley, C. S.; Čechal, J.; Kumagai, T.; Schramm, F.; Ruben, M.; Stepanow, S.; Kern, K. Highly Adaptable Two-Dimensional Metal–Organic Coordination Networks on Metal Surfaces. *J. Am. Chem. Soc.* **2012**, *134*, 6072–6075.

(5) Kudernac, T.; Lei, S. B.; Elemans, J. A. A. W.; De Feyter, S. Two-Dimensional Supramolecular Self-Assembly: Nanoporous Networks on Surfaces. *Chem. Soc. Rev.* **2009**, *38*, 402–421.

(6) De Feyter, S.; Miura, A.; Yao, S.; Chen, Z.; Wurthner, F.; Jonkheijm, P.; Schenning, A. P. H. J.; Meijer, E. W.; De Schryver, F. C. Two-Dimensional Self-Assembly into Multicomponent Hydrogen-Bonded Nanostructures. *Nano Lett.* **2005**, *5*, 77–81.

(7) Zhang, X. M.; Zeng, Q. D.; Wang, C. On-Surface Single Molecule Synthesis Chemistry: A Promising Bottom-Up Approach Towards Functional Surfaces. *Nanoscale* **2013**, *5*, 8269–8287.

(8) Bieri, M.; Nguyen, M. T.; Groning, O.; Cai, J. M.; Treier, M.; Ait-Mansour, K.; Ruffieux, P.; Pignedoli, C. A.; Passerone, D.; Kastler, M.; Mullen, K.; Fasel, R. Two-Dimensional Polymer Formation on Surfaces: Insight into the Roles of Precursor Mobility and Reactivity. *J. Am. Chem. Soc.* **2010**, *132*, 16669–16676.

(9) Perepichka, D. F.; Rosei, F. CHEMISTRY Extending Polymer Conjugation into the Second Dimension. *Science* **2009**, *323*, 216–217.

(10) Bonifazi, D.; Mohnani, S.; Llanes-Pallas, A. Supramolecular Chemistry at Interfaces: Molecular Recognition on Nanopatterned Porous Surfaces. *Chem.—Eur. J.* **2009**, *15*, 7004–7025.

(11) Cote, A. P.; Benin, A. I.; Ockwig, N. W.; O’Keeffe, M.; Matzger, A. J.; Yaghi, O. M. Porous, crystalline, covalent organic frameworks. *Science* **2005**, *310*, 1166–1170.

(12) El Garah, M.; MacLeod, J. M.; Rosei, F. Covalently Bonded Networks Through Surface-Confined Polymerization. *Surf. Sci.* **2013**, *613*, 6–14.

(13) Tanoue, R.; Higuchi, R.; Ikebe, K.; Uemura, S.; Kimizuka, N.; Stieg, A. Z.; Gimzewski, J. K.; Kunitake, M. In Situ STM Investigation of Aromatic Poly(azomethine) Arrays Constructed by “On-Site” Equilibrium Polymerization. *Langmuir* **2012**, *28*, 13844–13851.

(14) Zwaneveld, N. A. A.; Pawlak, R.; Abel, M.; Catalin, D.; Giggles, D.; Bertin, D.; Porte, L. Organized Formation of 2D Extended Covalent Organic Frameworks at Surfaces. *J. Am. Chem. Soc.* **2008**, *130*, 6678–6679.

(15) Marele, A. C.; Mas-Balleste, R.; Terracciano, L.; Rodriguez-Fernandez, J.; Berlanga, I.; Alexandre, S. S.; Otero, R.; Gallego, J. M.; Zamora, F.; Gomez-Rodriguez, J. M. Formation of a Surface Covalent Organic Framework Based on Polyester Condensation. *Chem. Commun.* **2012**, *48*, 6779–6781.

(16) Walch, H.; Dienstmaier, J.; Eder, G.; Gutzler, R.; Schlogl, S.; Sirtl, T.; Das, K.; Schmittel, M.; Lackinger, M. Extended Two-Dimensional Metal–Organic Frameworks Based on Thiolate–Copper Coordination Bonds. *J. Am. Chem. Soc.* **2011**, *133*, 7909–7915.

(17) Tanoue, R.; Higuchi, R.; Enoki, N.; Miyasato, Y.; Uemura, S.; Kimizuka, N.; Stieg, A. Z.; Gimzewski, J. K.; Kunitake, M. Thermodynamically Controlled Self-Assembly of Covalent Nano-architectures in Aqueous Solution. *ACS Nano* **2011**, *5*, 3923–3929.

(18) Weigelt, S.; Bombis, C.; Busse, C.; Knudsen, M. M.; Gothelf, K. V.; Lægsgaard, E.; Besenbacher, F.; Linderth, T. R. Molecular Self-Assembly from Building Blocks Synthesized on a Surface in Ultrahigh Vacuum: Kinetic Control and Topo-Chemical Reactions. *ACS Nano* **2008**, *2*, 651–660.

(19) Weigelt, S.; Busse, C.; Bombis, C.; Knudsen, M. M.; Gothelf, K. V.; Strunskus, T.; Woll, C.; Dahlbom, M.; Hammer, B.; Laegsgaard, E.; Besenbacher, F.; Linderth, T. R. Covalent Interlinking of an Aldehyde and an Amine on a Au(111) Surface in Ultrahigh Vacuum. *Angew. Chem., Int. Ed.* **2007**, *46*, 9227–9230.

(20) Yuan, Q. H.; Xing, Y. J.; Borguet, E. An STM Study of the pH Dependent Redox Activity of a Two-Dimensional Hydrogen Bonding

Porphyrin Network at an Electrochemical Interface. *J. Am. Chem. Soc.* **2010**, *132*, 5054–5060.

(21) Liao, L. Y.; Li, Y. B.; Zhang, X. M.; Geng, Y. F.; Zhang, J. Y.; Xie, J. L.; Zeng, Q. D.; Wang, C. STM Investigation of the Photoisomerization and Photodimerization of Stilbene Derivatives on HOPG Surface. *J. Phys. Chem. C* **2014**, *118*, 15963–15969.

(22) Takajo, D.; Inaba, A.; Sudoh, K. Two-Dimensional Solid-State Topochemical Reactions of 10,12-Pentacosadiyn-1-ol Adsorbed on Graphite. *Langmuir* **2014**, *30*, 2738–2744.

(23) Chen, M.; Xiao, J.; Steinruck, H. P.; Wang, S. Y.; Wang, W. H.; Lin, N.; Hieringer, W.; Gottfried, J. M. Combined Photoemission and Scanning Tunneling Microscopy Study of the Surface-Assisted Ullmann Coupling Reaction. *J. Phys. Chem. C* **2014**, *118*, 6820–6830.

(24) Fan, Q. T.; Wang, C. C.; Liu, L. M.; Han, Y.; Zhao, J.; Zhu, J. F.; Kuttner, J.; Hilt, G.; Gottfried, J. M. Covalent, Organometallic, and Halogen-Bonded Nanomeshes from Tetrabromo-Terphenyl by Surface-Assisted Synthesis on Cu(111). *J. Phys. Chem. C* **2014**, *118*, 13018–13025.

(25) Eichhorn, J.; Heckl, W. M.; Lackinger, M. On-Surface Polymerization of 1,4-Diethynylbenzene on Cu(111). *Chem. Commun.* **2013**, *49*, 2900–2902.

(26) Gao, H. Y.; Franke, J. H.; Wagner, H.; Zhong, D. Y.; Held, P. A.; Studer, A.; Fuchs, H. Effect of Metal Surfaces in On-Surface Glaser Coupling. *J. Phys. Chem. C* **2013**, *117*, 18595–18602.

(27) Zhang, X. M.; Liao, L. Y.; Wang, S.; Hu, F. Y.; Wang, C.; Zeng, Q. D. Polymerization or Cyclic Dimerization: Solvent Dependent Homo-Coupling of Terminal Alkynes at HOPG Surface. *Sci. Rep.* **2014**, *4*, 3899.

(28) Coratger, R.; Calmettes, B.; Abel, M.; Porte, L. STM Observations of the First Polymerization Steps between Hexahydroxy-Tri-Phenylene and Benzene-Di-Boronic Acid Molecules. *Surf. Sci.* **2011**, *605*, 831–837.

(29) Li, Y. B.; Wan, J. H.; Deng, K.; Han, X. N.; Lei, S. B.; Yang, Y. L.; Zheng, Q. Y.; Zeng, Q. D.; Wang, C. Transformation of Self-Assembled Structure by the Addition of Active Reactant. *J. Phys. Chem. C* **2011**, *115*, 6540–6544.

(30) Hu, F. Y.; Zhang, X. M.; Wang, X. C.; Wang, S.; Wang, H. Q.; Duan, W. B.; Zeng, Q. D.; Wang, C. In Situ STM Investigation of Two-Dimensional Chiral Assemblies through Schiff-Base Condensation at a Liquid/Solid Interface. *ACS Appl. Mater. Interfaces* **2013**, *5*, 1583–1587.

(31) Jensen, S.; Greenwood, J.; Fruchtl, H. A.; Baddeley, C. J. STM Investigation on the Formation of Oligoamides on Au{111} by Surface-Confined Reactions of Melamine with Trimesoyl Chloride. *J. Phys. Chem. C* **2011**, *115*, 8630–8636.

(32) Schmitz, C. H.; Schmid, M.; Gartner, S.; Steinruck, H. P.; Gottfried, J. M.; Sokolowski, M. Surface Polymerization of Poly(p-phenylene-terephthalamide) on Ag(111) Investigated by X-ray Photoelectron Spectroscopy and Scanning Tunneling Microscopy. *J. Phys. Chem. C* **2011**, *115*, 18186–18194.

(33) Xu, L. P.; Yan, C. J.; Wan, L. J.; Jiang, S. G.; Liu, M. H. Light-Induced Structural Transformation in Self-Assembled Monolayer of 4-(Amyloxy)Cinnamic Acid Investigated with Scanning Tunneling Microscopy. *J. Phys. Chem. B* **2005**, *109*, 14773–14778.

(34) Dienstmaier, J. F.; Gigler, A. M.; Goetz, A. J.; Knochel, P.; Bein, T.; Lyapin, A.; Reichlmaier, S.; Heckl, W. M.; Lackinger, M. Synthesis of Well-Ordered COF Monolayers: Surface Growth of Nanocrystalline Precursors versus Direct On-Surface Polycondensation. *ACS Nano* **2011**, *5*, 9737–9745.

(35) Liu, X. H.; Wang, D.; Wan, L. J. Surface Tectonics of Nanoporous Networks of Melamine-Capped Molecular Building Blocks formed through Interface Schiff-Base Reactions. *Chem-Asian J.* **2013**, *8*, 2466–2470.

(36) Elemans, J. A. A. W.; Lei, S.; De Feyter, S. Molecular and Supramolecular Networks on Surfaces: From Two-Dimensional Crystal Engineering to Reactivity. *Angew. Chem., Int. Ed.* **2009**, *48*, 7298–7332.

(37) Grill, L.; Dyer, M.; Lafferentz, L.; Persson, M.; Peters, M. V.; Hecht, S. Nano-Architectures by Covalent Assembly of Molecular Building Blocks. *Nat. Nanotechnol.* **2007**, *2*, 687–691.

(38) Saywell, A.; Schwarz, J.; Hecht, S.; Grill, L. Polymerization on Stepped Surfaces: Alignment of Polymers and Identification of Catalytic Sites. *Angew. Chem., Int. Ed.* **2012**, *51*, 5096–5100.

(39) Perepichka, D. F.; Rosei, F. Extending Polymer Conjugation into the Second Dimension. *Science* **2009**, *323*, 216–217.

(40) Guo, J.; Xu, Y. H.; Jin, S. B.; Chen, L.; Kaji, T.; Honsho, Y.; Addicoat, M. A.; Kim, J.; Saeki, A.; Ihee, H.; Seki, S.; Irle, S.; Hiramoto, M.; Gao, J.; Jiang, D. L. Conjugated Organic Framework with Three-Dimensionally Ordered Stable Structure and Delocalized pi Clouds. *Nat. Commun.* **2013**, *4*.

(41) Tehfe, M. A.; Dumur, F.; Graff, B.; Morlet-Savary, F.; Fouassier, J. P.; Gigmes, D.; Lalevee, J. New Push-Pull Dyes Derived from Michler's Ketone For Polymerization Reactions Upon Visible Lights. *Macromolecules* **2013**, *46*, 3761–3770.

(42) Guan, C. Z.; Wang, D.; Wan, L. J. Construction and Repair of Highly Ordered 2D Covalent Networks by Chemical Equilibrium Regulation. *Chem. Commun.* **2012**, *48*, 2943–2945.

(43) Chen, T.; Yan, H. J.; Yang, Z. Y.; Wang, D.; Liu, M. H. Assembling Structures of Barbituric Acid Derivatives on Graphite Surface Investigated with Scanning Tunneling Microscopy. *J. Phys. Chem. C* **2012**, *116*, 19349–19354.

(44) Yagai, S.; Kinoshita, T.; Higashi, M.; Kishikawa, K.; Nakanishi, T.; Karatsu, T.; Kitamura, A. Diversification of Self-Organized Architectures in Supramolecular Dye Assemblies. *J. Am. Chem. Soc.* **2007**, *129*, 13277–13287.

(45) Bohanon, T. M.; Denzinger, S.; Fink, R.; Paulus, W.; Ringsdorf, H.; Weck, M. Barbituric Acid/2,4,6-Triaminopyrimidine Aggregates in Water and Their Competitive Interaction with a Monolayer of Barbituric Acid Lipids at the Gas–Water Interface. *Angew. Chem., Int. Ed.* **1995**, *34*, 58–60.

(46) Ramondo, F.; Pieretti, A.; Gontrani, L.; Bencivenni, L. Hydrogen Bonding in Barbituric and 2-Thiobarbituric Acids: A Theoretical and FT-IR Study. *Chem. Phys.* **2001**, *271*, 293–308.

(47) Chen, T.; Yan, H. J.; Yang, Z. Y.; Wang, D.; Liu, M. H. Assembling Structures of Barbituric Acid Derivatives on Graphite Surface Investigated with Scanning Tunneling Microscopy. *J. Phys. Chem. C* **2012**, *116*, 19349–19354.

(48) Mahmudov, K. T.; Kopylovich, M. N.; Maharramov, A. M.; Kurbanova, M. M.; Gurbanov, A. V.; Pombeiro, A. J. L. Barbituric Acids as a Useful Tool for the Construction of Coordination and Supramolecular Compounds. *Coord. Chem. Rev.* **2014**, *265*, 1–37.

(49) Xie, R. S.; Song, Y. H.; Wan, L. L.; Yuan, H. Z.; Li, P. C.; Xiao, X. P.; Liu, L.; Ye, S. H.; Lei, S. B.; Wang, L. Two-Dimensional Polymerization and Reaction at the Solid/Liquid Interface: Scanning Tunneling Microscopy Study. *Anal. Sci.* **2011**, *27*, 129–138.

(50) Liu, X. H.; Guan, C. Z.; Ding, S. Y.; Wang, W.; Yan, H. J.; Wang, D.; Wan, L. J. On-Surface Synthesis of Single-Layered Two-Dimensional Covalent Organic Frameworks via Solid-Vapor Interface Reactions. *J. Am. Chem. Soc.* **2013**, *135*, 10470–10474.

(51) Cunha, F.; Tao, N. J. Surface-Charge Induced Order-Disorder Transition in an Organic Monolayer. *Phys. Rev. Lett.* **1995**, *75*, 2376–2379.

(52) Xu, L. R.; Zhou, X.; Yu, Y. X.; Tian, W. Q.; Ma, J.; Lei, S. B. Surface-Confined Crystalline Two-Dimensional Covalent Organic Frameworks via on-Surface Schiff-Base Coupling. *ACS Nano* **2013**, *7*, 8066–8073.

(53) Yoosaf, K.; Ramesh, A. R.; George, J.; Suresh, C. H.; Thomas, K. G. Functional Control on the 2D Self-Organization of Phenyleneethynyls. *J. Phys. Chem. C* **2009**, *113*, 11836–11843.

(54) Busse, C.; Weigelt, S.; Petersen, L.; Laegsgaard, E.; Besenbacher, F.; Linderoth, T. R.; Thomsen, A. H.; Nielsen, M.; Gothelf, K. V. Chiral Ordering and Conformational Dynamics for a Class of Oligo-Phenylene-Ethynyls on Au(111). *J. Phys. Chem. B* **2007**, *111*, 5850–5860.

(55) Maeda, Y.; Higuchi, T.; Ikeda, I. Change in Hydration State during the Coil-Globule Transition of Aqueous Solutions of Poly(N-

isopropylacrylamide) as Evidenced by FTIR Spectroscopy. *Langmuir* **2000**, *16*, 7503–7509.

(56) Sarafin, Y.; Birdilla, M.; Donio, S.; Velmurugan, S.; Michaelbabu, M.; Citarasu, T. Kocuria Marina BS-15 a Biosurfactant Producing Halophilic Bacteria Isolated from Solar Salt Works in India. *Saudi J. Biol. Sci.* **2014**, *21*, 511–519.

(57) Ibarra, J. V.; Munoz, E.; Moliner, R. FTIR Study of the Evolution of Coal Structure during the Coalification Process. *Org. Geochem.* **1996**, *24*, 725–735.

(58) Liu, Y.; Zhang, J.; Liu, Z.; Li, Z.; Yue, Z. Thermally Activated Polymerization Behavior of Bisphenol-S/Methylamine-Based Benzoxazine. *J. Appl. Polym. Sci.* **2012**, *124*, 813–822.

(59) Blazevska-Gilev, J.; Bastl, Z.; Subrt, J.; Stopka, P.; Pola, J. IR Laser Ablative Degradation of Poly(phenylene ether-sulfone): Deposition of Films Containing Ether, Sulfone, Sulfoxide and Sulfide Groups. *Polym. Degrad. Stab.* **2009**, *94*, 196–200.

(60) Inayama, S.; Mamoto, K.; Shibata, T.; Hirose, T. Structure and Antitumor Activity Relationship of 2-Arylidene-4-Cyclopentene-1,3-Diones and 2-Arylideneindan-1,3-Diones. *J. Med. Chem.* **1976**, *19*, 433–436.

(61) Meier, H.; Stalmach, U.; Kolshorn, H. Effective Conjugation Length and UV/vis Spectra of Oligomers. *Acta Polym.* **1997**, *48*, 379–384.